Earth and Planetary Science Letters 430 (2015) 398–407

Contents lists available at ScienceDirect

Earth and Planetary Science Letters

www.elsevier.com/locate/epsl

Crystallographic control on the boron isotope paleo-pH proxy

J. Noireaux [a,*], V. Mavromatis [b,1], J. Gaillardet [a], J. Schott [b], V. Montouillout [c], P. Louvat [a], C. Rollion-Bard [a], D.R. Neuville [a]

[a] Institut de Physique du Globe de Paris, Sorbonne Paris Cité, Université Paris Diderot, CNRS, F-75005 Paris, France
[b] Geosciences Environnement Toulouse (GET), CNRS, UMR5563, 14 Avenue Edouard Belin, 31400, Toulouse, France
[c] CEMHTI CNRS UPR3079, Univ. Orléans, 45071 Orléans cedex 1, France

ARTICLE INFO

Article history:
Received 15 April 2015
Received in revised form 17 July 2015
Accepted 29 July 2015
Available online 10 September 2015
Editor: H. Stoll

Keywords:
boron isotope
pH-proxy
synthetic calcite and aragonite
NMR

ABSTRACT

When using the boron isotopic composition ($\delta^{11}B$) of marine carbonates as a seawater pH proxy, it is assumed that only the tetrahedral borate ion is incorporated into the growing carbonate crystals and that no boron isotope fractionation occurs during uptake. However, the $\delta^{11}B$ of the calcium carbonate from most modern foraminifera shells or corals skeletons is not the same as the $\delta^{11}B$ of seawater borate, which depends on pH, an observation commonly attributed to vital effects. In this study, we combined previously published high-field ^{11}B MAS NMR and new $\delta^{11}B$ measurements on the same synthetic calcite and aragonite samples precipitated inorganically under controlled environments to avoid vital effects. Our results indicate that the main controlling factors of $\delta^{11}B$ are the solution pH and the mineralogy of the precipitated carbonate mineral, whereas the aqueous boron concentration of the solution, $CaCO_3$ precipitation rate and the presence or absence of growth seeds all appear to have negligible influence. In aragonite, the NMR data show that boron coordination is tetrahedral (BO_4), in addition, its $\delta^{11}B$ is equal to that of aqueous borate, thus confirming the paleo-pH hypothesis. In contrast, both trigonal BO_3 and tetrahedral BO_4 are present in calcite, and its $\delta^{11}B$ values are higher than that of aqueous borate and are less sensitive to solution pH variations compared to $\delta^{11}B$ in aragonite. These observations are interpreted in calcite as a reflection of the incorporation of decreasing amounts of boric acid with increasing pH. Moreover, the fraction of BO_3 measured by NMR in calcite is higher than that inferred from $\delta^{11}B$ which indicates a coordination change from BO_4 to BO_3 upon boron incorporation in the solid. Overall, this study shows that although the observed differences in $\delta^{11}B$ between inorganic and biological aragonite are compatible with a pH increase at calcification sites, the B speciation and isotope composition of biological calcites call for a more complex mechanism of boron incorporation.

1. Introduction

Understanding how the acidity of the oceans has evolved through geological time is a major challenge in earth sciences. Knowledge of past ocean pH is required to constrain the secular evolution of atmospheric pCO_2 and explore the links between CO_2 and climate. Two decades ago, boron isotopes ratios ($^{11}B/^{10}B$, expressed as $\delta^{11}B$ in ‰) in marine carbonates were proposed as a proxy for use in reconstructing the oceanic paleo-pH (Vengosh et al., 1991; Hemming and Hanson, 1992), and many studies have applied this promising proxy since that time (e.g., Hönisch and Hemming, 2005; Foster, 2008; Paris et al., 2010; Douville et al., 2010; Rae et al., 2011). The boron paleo-pH theory relies on large isotope fractionation between the two aqueous boron species in seawater, i.e., boric acid $B(OH)_3$ and borate ion $B(OH)_4^-$, and on the relative distribution of these two species as a function of pH. The two species are related to pH by the boric acid dissociation constant, the apparent value of which in seawater ($S = 35‰$, $T = 25\,°C$) is $K^*_B = 10^{-8.6}$ (Dickson, 1990). The isotope fractionation between $B(OH)_3$ and $B(OH)_4^-$ favors enrichment of light isotopes (^{10}B) in the borate ions and is approximately 27‰ in seawater at 25 °C (Klochko et al., 2006; Nir et al., 2015). As a result, if only borate ions are incorporated in the carbonate crystals that form from seawater and their incorporation occurs without isotopic fractionation, as generally hypothesized, the $\delta^{11}B$ of marine carbonates (mainly foraminifera and corals) should record the pH of seawater from which they

* Corresponding author at: Institut de Physique du Globe de Paris, 1 rue Jussieu, 75005 Paris, France. Tel.: +33 1 83 95 74 39.
E-mail address: noireaux@ipgp.fr (J. Noireaux).
[1] Current address: Institute of Applied Geosciences, Graz University of Technology, Rechbauerstrasse 12, A-8010 Graz, Austria.

http://dx.doi.org/10.1016/j.epsl.2015.07.063
0012-821X/

were formed (Hemming and Hanson, 1992). This pH value can be calculated according to the equation:

$$\mathrm{pH} = pK^*_B - \log\left(\frac{\delta^{11}B_{sw} - \delta^{11}B_c}{\alpha_{3\text{-}4}\cdot\delta^{11}B_c - \delta^{11}B_{sw} + 1000\cdot(\alpha_{3\text{-}4}-1)}\right) \quad (1)$$

where the subscripts *sw* and *c* denote seawater and carbonate, respectively.

However, in apparent contradiction with these assumptions, most of the δ^{11}B measured in calcium carbonates from modern calcifying organisms are shifted toward higher values compared with the δ^{11}B of the borate ion in seawater. Culture experiments of foraminifera and corals show that although a relationship does exist between the δ^{11}B of the carbonate skeleton and seawater pH, universal correlation does not exist between the measured δ^{11}B and the solution pH. Each species appears to require a specific calibration (e.g., Hönisch et al., 2004; Trotter et al., 2011; Anagnostou et al., 2012; Henehan et al., 2013). The most frequently invoked reason for these high δ^{11}B values and for the species dependency is the increase of pH at the calcification sites due to such species-specific vital effects as photosynthesis or proton–cation exchange reactions (Hönisch et al., 2003; Rollion-Bard and Erez, 2010). The influence of pH elevation on δ^{11}B at the calcification sites has been further demonstrated by the micron-scale variability of δ^{11}B in foraminifera and in *L. pertusa* deep-sea coral, as evidenced by SIMS measurements (Blamart et al., 2007; Rollion-Bard and Erez, 2010). Recently, boron coordination in biogenic calcium carbonate has been investigated using ^{11}B Magic Angle Spinning Nuclear Magnetic Resonance (^{11}B MAS NMR), and it has been shown that boron can exist in either a trigonal (BO_3) or tetrahedral form (BO_4). For example, the micro-scale spatial variability of δ^{11}B in *L. pertusa* coral has been attributed to variations in proportions of BO_3 and BO_4 incorporation (as measured by ^{11}B MAS NMR) detected in the various microstructure zones of the coral (Rollion-Bard et al., 2011a). The presence of BO_3 in the biogenic carbonates of corals and foraminifera (Klochko et al., 2009; Rollion-Bard et al., 2011a; Branson et al., 2015) challenges the assumption of preferential uptake of borate ion by calcium carbonates on which the boron pH proxy is based. In this respect, although co-precipitation and adsorption are distinct processes, previous studies have shown that both boric acid and the borate ion were adsorbed onto humic acids (Lemarchand et al., 2005) and iron or manganese oxides (Lemarchand et al., 2007) from experimental solutions. The δ^{11}B of sorbed boron was found to be pH dependent and controlled by the speciation of boron both in the solution and by the different complexes formed at the solid surface.

To circumvent the complexity induced by vital effects, the first step towards understanding boron incorporation mechanisms is the precipitation of inorganic carbonates with boron. Several authors have performed inorganic boron co-precipitation experiments with calcite or aragonite, but their results are contradictory. For example, the δ^{11}B values of calcite crystals grown by Sanyal et al. (2000) are shifted toward lower values (2–3‰) compared with the δ^{11}B values of the carbonate crystals (calcite, aragonite, high Mg-calcite) grown by Hemming et al. (1995). These conflicting results call for a better understanding of the mechanisms that control δ^{11}B in inorganic calcium carbonates over a wide range of pH and crystallization rates. In the current study, we analyzed a subset of the calcite and aragonite samples synthesized in Mavromatis et al. (2015), which covers a large range of pH values (pH 7 to 9.4), boron aqueous concentrations (0.4 mM to 20 mM) and $CaCO_3$ precipitation rates (2.3×10^{-8} mol/m^2/s to 6.8×10^{-6} mol/m^2/s). These samples were obtained by controlled boron co-precipitation with $CaCO_3$ using a method successfully developed to investigate magnesium isotope fractionation (Mavromatis et al., 2013). The boron partition coefficients between solution and solids and ^{11}B MAS NMR spectra were previously published in Mavromatis et al. (2015). In this work, the boron speciation and isotope ratios in the precipitated carbonates were characterized using high-resolution ^{11}B MAS NMR and MC-ICP-MS analyses, respectively.

This study shows that the mechanisms of boron co-precipitation are different in aragonite and in calcite, thus highlighting a strong crystallographic control on boron isotope fractionation. Although the δ^{11}B values measured in aragonite agree well with those of aqueous borate δ^{11}B in solution, δ^{11}B measured in calcite is shifted compared with the expected δ^{11}B of aqueous borate. In calcite, the dependence on solution pH of δ^{11}B is weaker than in aragonite. Isotopic data suggest the incorporation of both trigonal and tetrahedral boron into calcite.

2. Materials and methods

2.1. Experimental set-up

Boron co-precipitation with calcite and aragonite was performed using mixed flow reactors as described in Mavromatis et al. (2015). Precipitation occurred in a thermally-controlled 1 L sealed beaker in which pCO_2 and pH were held constant by continuous pumping of two inlet solutions and bubbling of a N_2/CO_2 gas mixture of known composition. A Teflon stir bar rotating at 120–150 rpm ensured the homogeneity of the reactive solution. The precipitation rate could be modified by changing the reactant concentrations in the inlet solutions and/or the pumping flow rate. All experiments were performed at 25 °C (±0.5 °C) in a 0.1 M or 0.2 M NaCl solution for 10 to 14 days. At the beginning of the experiment, 500 mL of a $NaCl/H_3BO_3$ solution were introduced to the reactor and allowed to equilibrate with the pCO_2 of the experiment. The simultaneous pumping of the two input solutions (i.e., a $CaCl_2$ solution and a Na_2CO_3/H_3BO_3 mixed solution) induced $CaCO_3$ precipitation. The concentrations of the $CaCl_2$ and Na_2CO_3 solutions ranged from 0.05 M to 0.1 M depending on the precipitation rate and the requested pH. The boric acid concentration in the inlet solution was equal to double that initially present in the reactor. The precipitation experiments were performed with a boron concentration in the reactor (parent solution) between 0.4 mM and 20 mM (Table S1). Both seeded and unseeded experiments were performed for calcite precipitation. Before the seeded experiments began, the calcite seeds (inorganic boron-free synthetic calcite) were allowed to equilibrate with the initial solution for 24 h. Aragonite was precipitated in unseeded experiments only. Precipitation of aragonite was induced by the presence of 0.025 M $MgCl_2$. The reactor solution was sampled each day to maintain constant the volume of the reactor (within 4%) and to measure the evolution of boron, calcium and alkalinity concentrations and δ^{11}B. The pH was measured *in situ*. At the end of an experiment, the entire solution was filtered through a 0.22-μm cellulose acetate Millipore filter, and the solids were rinsed twice with Milli-Q water and dried at room temperature. The XRD measurements indicate that the precipitate recovered at the end of each run consisted of a single $CaCO_3$ polymorph, aragonite or calcite (Mavromatis et al., 2015). The surface areas of the solids were determined by multi-point krypton adsorption according to the BET method. $CaCO_3$ growth rates at steady state were deduced from the balance between inlet and outlet calcium in the reactor during a given period of time, divided by the solids surface area (Mavromatis et al., 2015).

2.2. Analytical procedure

2.2.1. Major elements and pH

The calcium concentrations were measured by flame Atomic Absorption Spectroscopy (AAS) using a Perkin Elmer AAnalyst

400 instrument with an uncertainty of ±1% and a detection limit of 7×10^{-7} M. Alkalinity was determined following a standard HCl titration procedure using an automatic Schott TitroLine alpha TA10plus titrator with an uncertainty of ±2% and a detection limit of 5×10^{-7} M. The pH was measured *in situ* using a Mettler Toledo combined electrode calibrated on the activity scale with NIST buffers (pH = 4.006, 6.865 and 9.183 at 25 °C). Differences in liquid-junction potentials between NIST buffers and experimental solutions never exceeded 1 mV, as calculated using data reported by Bates (1973). The precision of the pH measurements was ±0.02 units (1 mV), and the pH variation during each precipitation experiment was less than 0.05 pH units.

2.2.2. Boron isotope and concentration measurements

Prior to δ^{11}B measurements, boron was chemically separated from the solid or the solution to obtain a final solution containing only boron in a diluted nitric acid solution (HNO_3 = 0.05 M). The extraction procedures were slightly different for solids and for aqueous solutions. Typically for solids, 5 mg to 20 mg of calcium carbonate was dissolved in 0.5 M HNO_3 and ultrasonicated for 30 min in a closed Teflon beaker. Boron was extracted using two-step separation chemistry. The solution was first loaded on a 300-µL DIONEX AG 50-X8 cation-exchange column to remove the calcium matrix. Next, the pH of the solution was adjusted to 8–9 with a pre-distilled ammonia solution. The solution was subsequently loaded on a chromatography column that contained 10 µL of the boron-specific Amberlite IRA 743 resin. The detailed procedure steps for these columns can be found in Louvat et al. (2010). To extract boron from the precipitation solution, only the 10-µL Amberlite IRA 743 column was used because a notably small amount of solution was required (approximately 50 µL) to reach the boron amount for isotope measurements. The δ^{11}B were measured by bracketing with the NIST 951 standard solution on a MC-ICP-MS Neptune using a d-DIHEN (demountable-Direct Injection High Efficiency Nebulization) sample introduction system. The detailed bracketing technique and the d-DIHEN automation set-up specifically designed to measure the δ^{11}B are described in Louvat et al. (2010, 2014). The long-term reproducibility of our measurements is 0.2‰ (two standard deviations, 2σ), as estimated based on two-year measurements of boron in-house enriched standard (SE43). The accuracy of our method for carbonates was estimated by measuring coral sample COM-4, for which we found a value of 24.6 ± 0.3‰ (n = 4), consistent with the previous measurements from Louvat et al. (2010) and by participating to an inter-laboratory comparison of δ^{11}B in marine $CaCO_3$ (Foster et al., 2013). Most solid samples were measured at least twice (after two independent dissolutions followed by boron extraction). The δ^{11}B of the solution was −0.8 ± 0.4‰, and its variation during one experiment was less than 0.3‰. The total blank of the chemical procedure was 0.24 ng (n = 9) and was thus considered negligible compared to the amount of boron analyzed (50 ng to 200 ng of boron). Boron concentrations were determined either directly by MC-ICP-MS after the chemical separation detailed above or by a Horiba Jobin Yvon Ultima2 ICP-OES over a concentration range of 1.5–46.7 × 10^{-6} M with an uncertainty of <2%. The reproducibility of boron concentrations was ±3% for solutions and ±8% for solid phases.

2.3. Speciation calculations

Aqueous speciation and the saturation state Ω of the reacting solution with respect to calcite and aragonite were calculated using the PHREEQC software together with its MINTEQA2 database (Parkhurst and Appelo, 2013). This model calculates the activity coefficients of free aqueous ions and charged complexes using the Davies equation. The value for the boric acid hydrolysis constant was taken from Baes and Mesmer (1976). The values of the formation constants for $MgB(OH)_4^+$ and $CaB(OH)_4^+$ ion pairs were taken from the NIST database (Martell et al., 2004), whereas that for the $NaB(OH)_4^\circ$ ion pair was taken from Pokrovski et al. (1995). Table S2, which reports the calculated boron aqueous speciation in our experimental solutions, shows that the proportion of $CaB(OH)_4^+$ is always negligible (<0.8%), whereas $NaB(OH)_4^\circ$ represents up to 2% and 7.7% of total B in the 0.1 M and 0.2 M NaCl solutions, respectively. Depending on pH, the $MgB(OH)_4^+$ ion pair represents between 1% and 9% of total B in aragonite-forming solutions. Additionally, we note that similar boron aqueous speciation is obtained using the Pitzer module implemented in PHREEQC except for $NaB(OH)_4^\circ$, which is not identified in the Pitzer specific interaction approach (see Table S2).

3. Results

3.1. Boron isotope composition and speciation in carbonates

In aragonite samples, the δ^{11}B values range from −25.0‰ to −14.7‰ and exhibit ^{11}B depletion compared with the parent solution ($\delta^{11}B = -0.8 \pm 0.3$‰). Aragonite shows a systematic increase in δ^{11}B with increasing pH (Fig. 1a). Calcite samples show a lower range of δ^{11}B with values between −17.5‰ to −11.0‰ and are also depleted in ^{11}B compared with the parent solution (Fig. 1b). As in aragonite, the δ^{11}B in calcite also increases with pH (except for the experiment conducted at pH 9.39, Fig. 1), but at a given pH, the δ^{11}B are much higher than in aragonite. For example, at pH 8.3, calcite is enriched in ^{11}B by approximately 7‰ compared with aragonite. The calcite precipitated at pH 9.39 is an outlier that will not be taken in account in the following discussion. The δ^{11}B of this sample lies much lower that the general trend of the other calcites and has a larger uncertainty on its δ^{11}B. This could be du to some experimental problems, for example at this high pH, the precipitation starts before the complete homogenization of the solution.

The SEM imaging of a few samples (Fig. 3 in Mavromatis et al., 2015) did not permit detection of fluid inclusions, which could have accounted for these high δ^{11}B values in calcite. Furthermore, the δ^{11}B increase when pH rises from 7.5 to 8.9 is much smaller in calcite (+6.5‰) than in aragonite (+10.3‰). Our data clearly confirm that the solution pH controls the variations of δ^{11}B in aragonite and calcite, but the nature of the carbonate polymorph exerts a primary control both on the magnitude of the boron isotope fractionation between the calcium carbonate and the parent solution and on the slope of the δ^{11}B increase with pH.

Fig. 2 presents an example of ^{11}B MAS NMR spectra of calcite and aragonite precipitated at pH 8.6. It can be observed that at this pH value, boron speciation is radically different between calcite and aragonite. In calcite, both the BO_3 and BO_4 forms are present in equivalent proportions (60% BO_3 and 40% BO_4), whereas in aragonite, BO_4 is largely dominant. Estimates of the BO_3 and BO_4 proportions for all precipitates characterized in this study using ^{11}B MAS NMR are listed in Table 1. In aragonite, BO_4 is the dominant form at all investigated pH values, from 85% to 100% with an average of 91% of the total boron. In contrast, in calcite, boron speciation is highly variable with BO_4 accounting for 35% to 85% of total boron (Table 1). Boron speciation in calcite or aragonite is not correlated with the pH of the precipitating solution or with the concentration of boron in the solid.

3.2. Effects of the precipitation parameters on boron isotope fractionation

Because NMR exploration requires a minimum of 12 ppm B content in solids and because of the relatively low affinity of

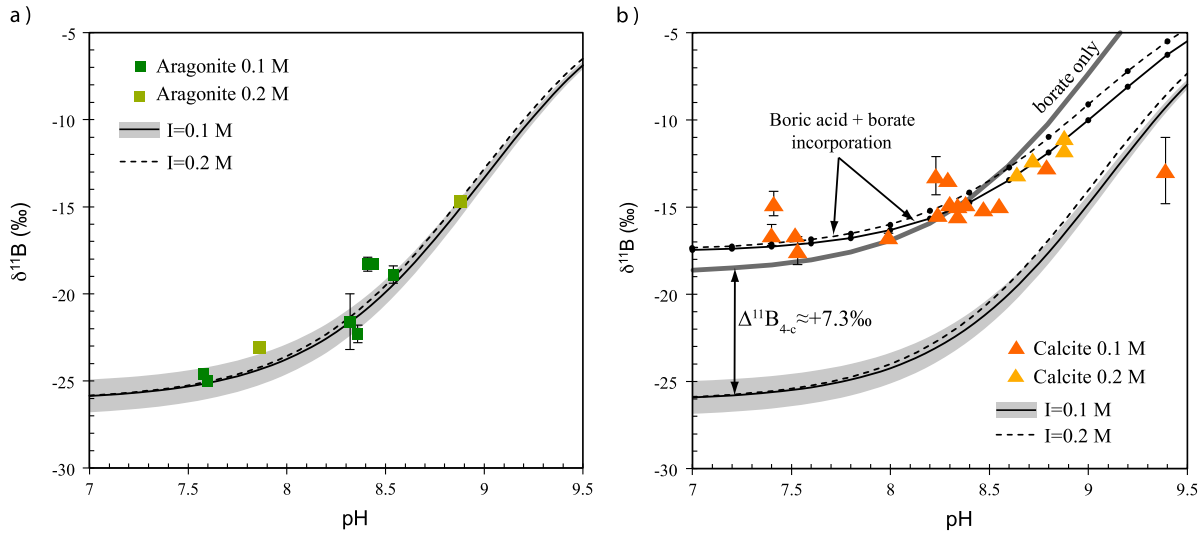

Fig. 1. δ^{11}B measurements vs. pH for aragonite (a) and calcite (b). The δ^{11}B curves for borate (plain and dotted black lines) were calculated for two ionic strengths ($I = 0.1$ M and $I = 0.2$ M) using a fractionation factor α_{3-4} value of 1.026 ± 0.001 (Nir et al., 2015), and the borate concentrations were obtained from PHREEQC modeling (see Method section). The grey area indicates the error associated with the α_{3-4} value for a $I = 0.1$ M precipitation solution. In Fig. 1b, the curves with black circles (plain for I = 0.1 M, dotted for $I = 0.2$ M) display a fit of the data corresponding to the incorporation of both boric acid and borate with no isotopic fractionation (deduced from Fig. 6). The grey line denotes the model fitted for borate incorporation with an isotopic fractionation factor $\alpha_{4\text{-}C}$, of 0.993 (or +7.3‰). The results shown in this figure cover the entire range of experimental conditions of the current study (precipitation rates, boron concentrations, experiments with and without seeds).

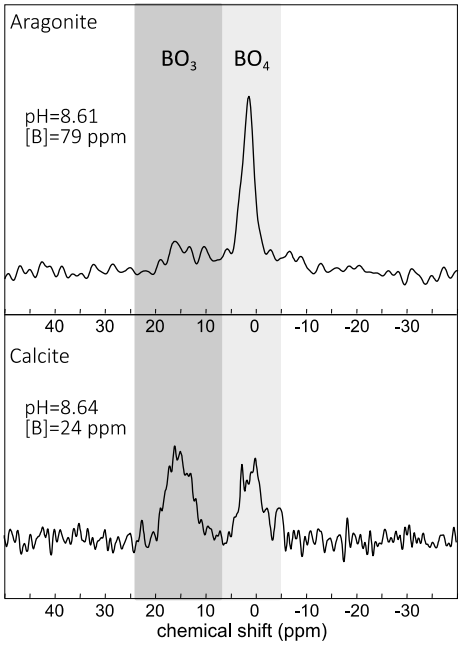

Fig. 2. ^{11}B MAS NMR spectra of aragonite and calcite at pH 8.6. ($\nu_{RF} = 272.8$ MHz, MAS speed = 20 kHz). Data from Mavromatis et al. (2015).

boron for carbonates, we performed precipitation experiments with boron concentrations in solution ranging from that of seawater (0.45 mM) up to 20 mM. This range allowed us to test the influence of B concentration in solution on the measured δ^{11}B of carbonates (Figs. 3a, 3b). For the range of B concentrations explored in this study at a constant pH, we observe no systematic δ^{11}B variation with B concentration, neither for aragonite nor for calcite. Because the precipitation rate has been shown to affect the isotopic composition of divalent metal traces co-precipitated with calcite or aragonite (i.e., Sr^{2+}, Tang et al., 2008; Ba^{2+}, Von Allmen et al., 2010; Mg^{2+}, Mavromatis et al., 2013), we conducted our experiments at various precipitation rates (Figs. 3c, 3d). Surface normalized precipitation rates were varied from 2.3×10^{-8} mol/m^2/s to 6.8×10^{-6} mol/m^2/s, which covers the range of reported precipitation rates for biogenic calcite and aragonite (Gussone et al., 2005; McCulloch et al., 2012). Fig. 3 shows that the precipitation rate does not induce any systematic variations of the δ^{11}B of calcite and aragonite, although it was shown that the amount of incorporated boron increases with the precipitation rate in the same samples (Mavromatis et al., 2015).

Table 1
Proportion of trigonal boron (BO_3) and tetrahedral (BO_4) boron measured by ^{11}B MAS NMR in calcite and aragonite samples. Numbers in parentheses denote the uncertainties (in %); n.d. = not determined. Data are reported from Mavromatis et al. (2015).

N°	Mineralogy	pH	rate mol/m^2/s	BO_3 (%)	BO_4 (%)
8	Calcite	7.52	3.2E−06	65 (±20)	35 (±20)
111	Calcite	7.99	6.8E−06	15 (±10)	85 (±10)
12	Calcite	8.34	2.9E−06	60 (±10)	40 (±10)
46	Calcite	8.64	3.4E−06	60 (±15)	40 (±15)
85	Calcite	8.88	6.6E−06	23 (±20)	77 (±20)
9	Aragonite	7.58	n.d.	15 (±5)	85 (±5)
27	Aragonite	8.61	1.1E−06	0 (±5)	100 (±5)
87	Aragonite	8.88	8.5E−07	13 (±5)	87 (±5)

We also compared the impact of precipitation on calcite homogeneous nucleation (unseeded runs) and heterogeneous nucleation (with seeds). The surface-normalized precipitation rate of calcite obtained in the presence of seed material is approximately two orders of magnitude lower compared with experiments performed without seeds (Table S1). This situation likely results from the need to overcome the energy barrier that inhibits $CaCO_3$ nucleation and from the higher solution saturation states required to initiate precipitation in unseeded runs (e.g., Dandurand et al., 1982). However, it can be observed in Fig. 4 that at a given pH, the calcite δ^{11}B values are the same (within uncertainties) for the unseeded and seeded experiments. This result demonstrates that homogeneous and heterogeneous nucleation runs are both suitable for characterizing boron isotope fractionation between calcite and solution.

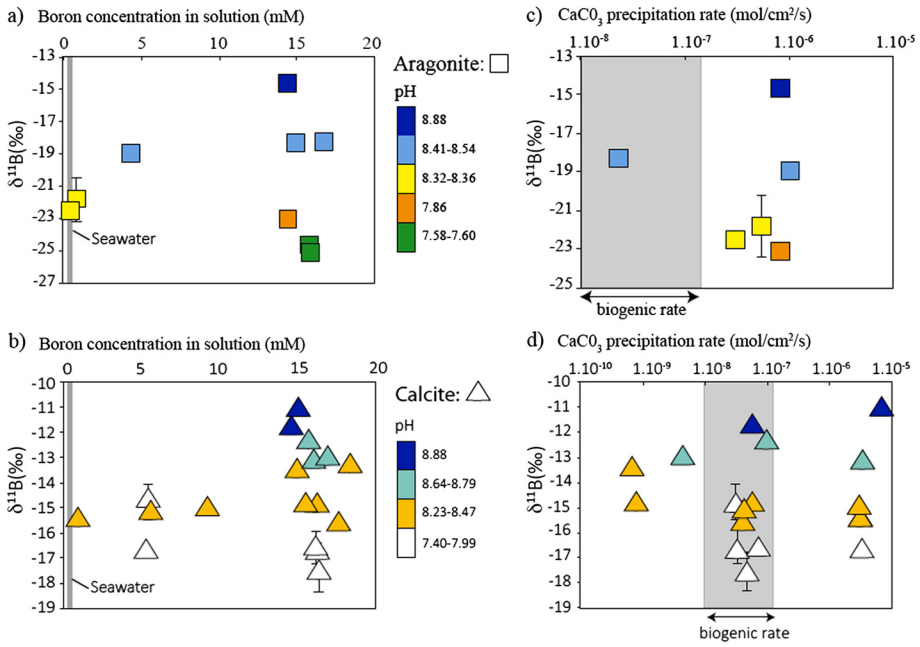

Fig. 3. Influence of the aqueous boron concentration and the precipitation rate on the boron isotopic composition of aragonites (a and c) and calcites (b and d). The pH values of the experiments are shown in the grey color scale. The range of precipitation rates of biogenic carbonates (Gussone et al., 2005; McCulloch et al., 2012) and the boron concentration in seawater are added for comparison.

4. Discussion

4.1. Boron aqueous speciation and isotopic composition of boron species

To properly interpret the previously described experimental results, the speciation of aqueous boron and the $\delta^{11}B$ of the different species must be known. In seawater, most studies on boron isotopes consider that boron is present as two main species, i.e., boric acid ($B(OH)_3$) and borate ion ($B(OH)_4^-$). The boric acid apparent hydrolysis constant determined at 25 °C in seawater by Dickson (1990) is generally used to calculate boron aqueous speciation. Recently, Nir et al. (2015) used the Specific Ion Interaction theory (Pitzer, 1973), which recognizes the formation of $MgB(OH)_4^+$ and $CaB(OH)_4^+$ ion pairs, to calculate boron speciation in solutions of several salinities. Because the precipitation experiments of the current study were performed in NaCl solutions of much lower ionic strengths than that of seawater (from 0.1 M to 0.2 M), the formation of the borate ion pairs must be explicitly taken into account (see the Methods section and Table S2). The value of the isotopic fractionation factor between boric acid and borate (hereafter denoted α_{3-4}) has been the subject of debates, but it is now well constrained, and the value of $\alpha_{3-4} = 1.0272 \pm 0.0006$ at 25 °C as determined by Klochko et al. (2006) in synthetic seawater ($I = 0.7$ M) is currently the most frequently used for paleo-pH reconstructions. Two other values were determined in the same study in 0.6 M KCl ($\alpha_{3-4} = 1.0250 \pm 0.0005$) and pure water ($\alpha_{3-4} = 1.0308 \pm 0.0023$). Recently, Nir et al. (2015) used a reverse osmosis membrane to separate boric acid and found $\alpha_{3-4} = 1.026 \pm 0.001$ ($\varepsilon = 26.0 \pm 1.0$‰) in solutions of various salinities. In Fig. 1a, b, using the α_{3-4} of Nir et al. (2015), we plotted the expected $\delta^{11}B$ of aqueous borate as a function of pH calculated as the sum of the free borate and the Mg, Ca and Na borate ion pairs. In the absence of literature data, we assumed that the Mg-, Ca-, Na-borate ion pairs in solution exhibit the same isotope fractionation as the free borate ion with respect to boric acid. This assumption is justified by the fact that boron is tetrahedral in the ion pairs with Ca, Na and Mg and is supported by the similarity (within errors) of the α_{3-4} values determined in seawater,

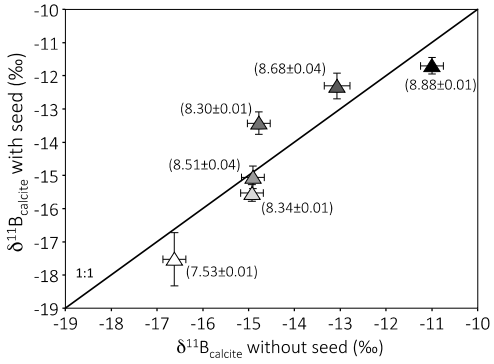

Fig. 4. Comparison of $\delta^{11}B$ in calcites precipitated with or without seeds. Each point is the comparison between $\delta^{11}B$ of two calcites precipitated at approximately the same pH value, one experiment performed with seed and one without seed. The number next to each symbol corresponds to the pH of the experiment.

0.6 M KCl and other more diluted solutions (Klochko et al., 2006; Nir et al., 2015). It can be observed in Fig. S1 that taking into account the Mg ion pairing in aragonite parent solutions results in a slight increase (up to 1.5‰ at pH 9) of the $\delta^{11}B$ for aqueous borate compared with that of the calcite experiments.

4.2. Comparison of boron isotopic fractionation with previous inorganic precipitation experiments

Several previously published experiments investigated the inorganic co-precipitation of boron in calcite and aragonite. The $\delta^{11}B$ of calcite and aragonite measured in our study are compared with $\delta^{11}B$ obtained by Hemming et al. (1995) and Sanyal et al. (2000) in a plot of $\delta^{11}B_{CaCO3}-\delta^{11}B_{sol}$, (the $\delta^{11}B$ difference between carbonate and parent solution) vs. $\delta^{11}B_4-\delta^{11}B_{sol}$ (the $\delta^{11}B$ difference between aqueous borate and parent solution) calculated for each parent solution (Fig. 5). Similar to our results, Mg-free calcites from Hemming et al. (1995) and Sanyal et al. (2000) are enriched in ^{11}B compared with the aqueous borate, showing that this offset exists despite the different compositions of the parent solution among

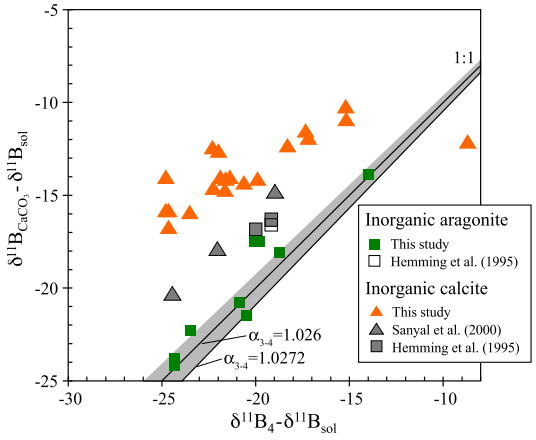

Fig. 5. Comparison between the present $\delta^{11}B$ of inorganic carbonates and published values. The experiments from Sanyal et al. (2000) and from Hemming et al. (1995) were precipitated in solutions of different isotope composition and different compositions. The isotope fractionation is thus plotted as the difference between $\delta^{11}B$ measured in carbonates and the $\delta^{11}B$ in the parent solution ($\delta^{11}B_{CaCO3}-\delta^{11}B_{sol}$). The $\delta^{11}B$ of borate was calculated for each experiment (using α_{3-4} from Nir et al., 2015) and expressed as the difference between the $\delta^{11}B$ of borate and the $\delta^{11}B$ of the parent solution ($\delta^{11}B_4-\delta^{11}B_{sol}$).

the three studies ($CaCl_2$–NH_3Cl with Mg for aragonite precipitation in Hemming et al. (1995), Mg-free seawater in Sanyal et al. (2000), NaCl–$CaCl_2$ with Mg for aragonite in the current study). However, control of $\delta^{11}B$ by the nature of the precipitated $CaCO_3$ polymorphs that is evidenced in the current study was not detected in the study of Hemming et al. (1995). Several explanations are possible for these contrasting results. First, Hemming et al. (1995) only performed two experiments, one leading to the precipitation of a pure Mg-free calcite and the other producing a mix of aragonite and high-Mg calcite. It is thus possible that the measured $\delta^{11}B$ of this latter mixture was not representative of pure aragonite or pure high-Mg calcite end-members. Second, the precipitation protocol used by these authors was a free-drift technique, leading to large differences between the initial and the final pH (up to 3 pH units). Sanyal et al. (2000) argued that in such a set-up, a pH gradient could be responsible for the shift in $\delta^{11}B$ between their precipitated calcites and those of Hemming et al. (1995). A +2 to +4‰ offset is also observed between our results and those of Sanyal et al. (2000) for calcite. Hönisch et al. (2003) previously observed a constant +2.7‰ offset between their measurements and those from Sanyal et al. (1996). They attributed this shift to analytical issues potentially related to the TIMS technique and to matrix effects between standards and samples. Similar causes may explain the discrepancy between our measurements and those from Sanyal et al. (2000), although the composition of the precipitation solution composition may also play a role.

4.3. Mechanism of boron incorporation into aragonite

The rather distinct boron speciation and $\delta^{11}B$ in calcite and aragonite suggests that the boron incorporation mechanisms are different. In Fig. 1a, we plotted the measured $\delta^{11}B$ of precipitated aragonite as a function of pH as well as the $\delta^{11}B$ of aqueous borate (calculated as explained in Section 4.1). Except for two points (pH 8.41 and 8.44), which are slightly shifted to higher $\delta^{11}B$, our aragonite $\delta^{11}B$ values perfectly fall on the curve describing aqueous borate isotope composition as a function of pH. This agreement strongly supports the preferential incorporation of borate in aragonite without any isotope fractionation. This result validates the hypothesis of the paleo-pH boron proxy.

The NMR data show that BO_4 is by far the dominant species in aragonite and that the small amount of BO_3 is not correlated with the solution pH (Table 1). Assuming that aqueous boric acid and the borate ion are both incorporated into the crystal lattice without any isotope fractionation, it is possible to calculate the fraction of aqueous boric acid required ($BO_{3\text{-ISO}}$) to account for the shift between our measured $\delta^{11}B$ value of aragonite and the $\delta^{11}B$ of borate:

$$\delta^{11}B_{aragonite} = BO_{3\text{-ISO}}\delta^{11}B_{boric} + (1 - BO_{3\text{-ISO}})\delta^{11}B_{borate} \quad (2)$$

where $\delta^{11}B_{borate}$ and $\delta^{11}B_{boric}$ are the boron isotopic ratios of borate ion and boric acid in solution, respectively.

The values of $BO_{3\text{-ISO}}$ range between 0% and 0.1% for all samples between pH 7.58 and pH 8.88, based on Eq. (2) using $\delta^{11}B_{boric}$ and $\delta^{11}B_{borate}$ end-members. Comparatively, $BO_{3\text{-NMR}}$, the proportions of BO_3 measured by ^{11}B MAS NMR (Table 1) are $15 \pm 5\%$ at pH 7.58 and $13 \pm 5\%$ at pH 8.88. If such high BO_3 proportions were representative of boric acid incorporated in aragonite, then according to Eq. (2), the resulting $\delta^{11}B$ of aragonite would be higher than what is actually measured. The inconsistency between $BO_{3\text{-NMR}}$ and $BO_{3\text{-ISO}}$ implies that trigonal boron detected by ^{11}B MAS NMR does not directly derives from aqueous boric acid but is due to coordination change.

In agreement with Klochko et al. (2009), we suggest that the small proportions of measured BO_3 derive from aqueous tetrahedral boron that underwent a coordination change with no isotope fractionation during or after its incorporation in the aragonite lattice. From the solution to the aragonite lattice, the change of coordination therefore does not appear to induce any observable isotope fractionation. A similar conclusion was previously reached by Sen and Stebbins (1994) and Klochko et al. (2009). This surprising result might indicate that tetrahedral boron is not in contact with the parent solution when it undergoes a change in coordination.

As mentioned previously, two aragonite samples display slightly higher $\delta^{11}B$ than the borate curve. It is possible that despite all of our careful samples washing, a small amount of the parent solution remained at the solids surface, resulting in an increased $\delta^{11}B$. The incorporation of another boron species, i.e., boric acid or the fractionation of the borate ion during incorporation, is unlikely to explain this shift because these two samples were precipitated under similar conditions as the others (ionic strength and the same boron concentrations).

4.4. Mechanism of boron incorporation into calcite

In calcite, our results call for a strikingly different behavior of boron isotopes during co-precipitation (Fig. 1b and Fig. 2; Table 1). At all pH values (except at pH 9.39), the measured $\delta^{11}B$ of calcite is significantly enriched in ^{11}B compared with aqueous borate (Fig. 1b) and therefore does not fit the expected $\delta^{11}B$ of borate in solution. This result demonstrates that boron is not incorporated into calcite according to the hypothesis of exclusive aqueous borate incorporation with no isotope fractionation. Relative to aragonite, the NMR spectra show more significant proportions of BO_3 in the crystal lattice, but these proportions do not show any relationship with pH (Table 1). As a consequence, the proportion of BO_3 and BO_4 measured by NMR cannot reflect the proportions of aqueous boric acid and borate ion incorporated into the carbonate.

To interpret the results from Fig. 1b, we first consider the incorporation of borate into calcite with a constant isotope fractionation. The $\delta^{11}B$ of aqueous borate was first calculated for the calcite parent solution using a α_{3-4} of 1.026 ± 0.001 (see Section 4.1). Next, a constant isotope fractionation $\alpha_{4\text{-C}}$ was applied to aqueous borate during its incorporation into the crystal lattice (gray curve on Fig. 1b). Although a value of $\alpha_{4\text{-C}} = 0.993$ (or $\Delta^{11}B_{4\text{-C}} \approx +7.3$‰) explains the highest number of data points, it

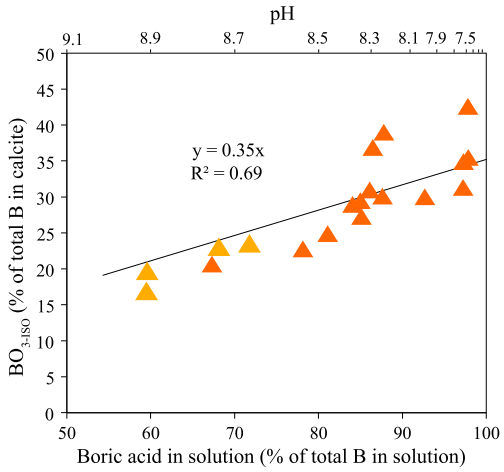

Fig. 6. Proportion of trigonal boron incorporated into calcite deduced from the $\delta^{11}B$ of calcite ($BO_{3\text{-ISO}}$) as a function of the proportions of boric acid and pH of the solution. It is assumed that the incorporation of aqueous boric acid in the solid does not fractionate the boron isotopes ($\alpha_{3\text{-c}} = 1$).

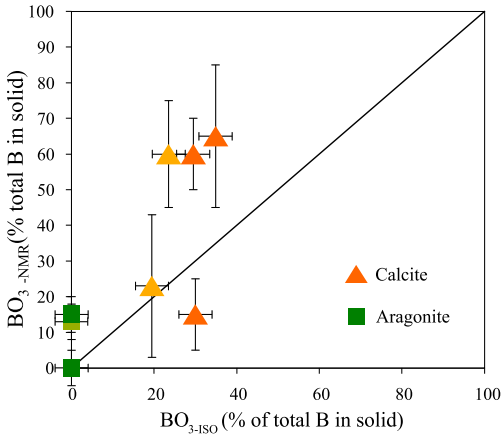

Fig. 7. Boron solid speciation in calcite and aragonite. Comparison between the proportions of BO_3 determined by NMR ($BO_{3\text{-NMR}}$) and by $\delta^{11}B$ in the solid, ($BO_{3\text{-ISO}}$), assuming no isotopic fractionation of boric acid or borate ion. The diagonal is indicated as a guide line.

fails to explain the values measured at pH > 8.5 (Fig. 1b). Conversely, a fractionation of +5‰ could account for the results at high pH values but fails to reproduce the low pH values (not shown). Hence, at least two different fractionation values for borate would be required to explain our calcite data assuming only aqueous borate is incorporated. Such situation would occur if borate exists in two different forms (two complexes or ion pairs with distinct isotope fractionation) whose relative proportions depend on pH. In the absence of any evidence for the existence of such complexes and because the magnitude of the change of coordination is not correlated with pH, we consider the alternative explanation that boric acid is incorporated in addition to borate into calcite. If we assume that boric acid and borate are incorporated into the crystal lattice with no isotope fractionation, it is possible to calculate the proportions of aqueous boric acid $BO_{3\text{-ISO}}$ that are incorporated into calcite (Eq. (2) applied to calcite). Calculated values of $BO_{3\text{-ISO}}$ in calcite range from 17% to 43% and appear to be linearly correlated with the fraction of boric acid in solution (Fig. 6). The decrease of the fraction of boric acid incorporated into calcite with increasing pH is thus related to the abundance of boric acid in solution. This model satisfactorily reproduces the measured calcite $\delta^{11}B$ at high pH and the decrease in the sensitivity of the $\delta^{11}B$ vs. pH relationship (Fig. 1b).

As shown on Fig. 7, the proportions of boric acid given by NMR ($BO_{3\text{-NMR}}$) are significantly higher than those derived from Eq. (2) ($BO_{3\text{-ISO}}$), assuming no isotope fractionation during incorporation. This result suggests that a significant proportion of calcite boron has undergone a change from tetrahedral to trigonal coordination during its incorporation into the lattice (similar to aragonite). In this case, the boron coordination change was not accompanied by an isotopic fractionation. Such a change of coordination of borate without isotopic fractionation can be understood if the coordination change occurs when boron is isolated from the solution. It has been previously invoked to explain the NMR and isotopic data on boron inorganically co-precipitated with calcite at pH = 8 (Sen and Stebbins, 1994). Such a coordination change was also proposed from NMR investigations in biological coral and foraminifera carbonates in both aragonite and calcite (Klochko et al., 2009; Branson et al., 2015). The absence of a direct relationship between the proportion of estimated aqueous boric acid incorporated into calcite (pH dependent) and the proportion measured in calcite by NMR together with the decrease of the BO_3 proportions in the lattice from 60% to 15% when calcite precipitation rate increases from 2.9×10^{-6} mol/m^2/s to 6.8×10^{-6} mol/m^2/s at similar pH values (Table 1) suggest that the amplitude of B coordination change decreases with calcite growth rate. The faster the calcite grows, the less time is available for boron to change its coordination and the more tetrahedral B can be incorporated in the solid (Ruiz-Agudo et al., 2012). However, as suggested by the ab initio calculations of the $\delta^{11}B$ of trigonal corner-sharing B-carbonate complexes (Tossell, 2006), it cannot be ruled out that calcite trigonal boron incorporated in the solid could be isotopically lighter than aqueous boric acid. Fractionation between aqueous boric acid and incorporated trigonal boron would imply that the proportions of boric acid incorporated should be even higher, which would lower the fraction of BO_3 in calcite derived from borate undergoing a coordination reduction upon incorporation into the lattice.

This conceptual model is consistent with the following assumptions: 1) the preferential incorporation of borate in $CaCO_3$ growth sites for both calcite and aragonite and 2) the existence of an energy barrier for tetrahedral boron to enter the calcite lattice, leading to a reduction of B coordination number. This energy barrier hampers B uptake in calcite and explains the smaller boron concentrations observed in this mineral compared with aragonite (Table S1; Sen and Stebbins, 1994; Mavromatis et al., 2015). In a parallel study, Mavromatis et al. (2015) showed that the rate at which calcite and aragonite were precipitated exerts major control on the B partition coefficient in these two carbonates. The impact of precipitation rate on the boron partition coefficient in calcite was confirmed in recent inorganic experiments by Gabitov et al. (2014) and Uchikawa et al. (2015). However, calcite and aragonite boron isotopic compositions were not observed to depend on the solid precipitation rates investigated in the current study and pH remains the major control on the boron isotope composition of the aragonite and calcite.

4.5. Comparison with biological carbonates

Since the pioneering papers of Vengosh et al. (1991) and Hemming and Hanson (1992), a large number of studies have analyzed $\delta^{11}B$ in biogenic carbonates to determine the paleo-pH of the ocean. Corals (surface and deep sea) and foraminifera (planktonic and benthic), both aragonitic and calcitic, were mostly used for this purpose. A number of calibration curves between seawater pH and the $\delta^{11}B$ of the carbonates shells were constructed based on culture experiments under controlled conditions. These data do show a dependency of $\delta^{11}B$ with culture pH but are often offset toward higher $\delta^{11}B$ compared with the theoretical curve of bo-

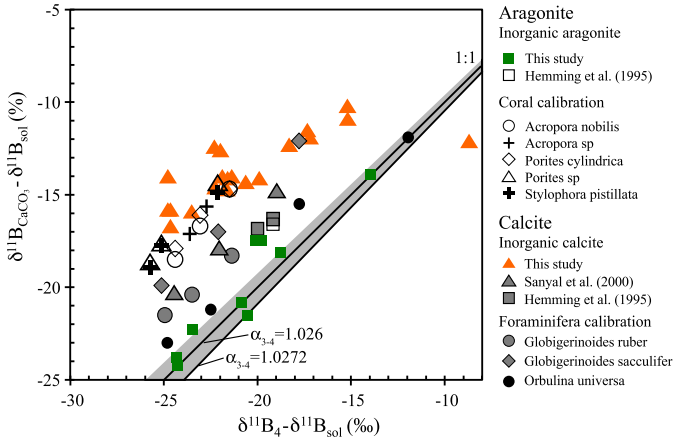

Fig. 8. Comparison with laboratory calibrations of corals (aragonite) and foraminifera (calcite). The data for tropical corals grown in controlled environments for *Acropora Nobilis* and *Porites Cylindrica* are taken from Hönisch et al. (2004); data for *Acropora sp.* are taken from Reynaud et al. (2004); and *Porites sp.* and *Stylophora pistillata* data are taken from Krief et al. (2010). The data for foraminifera grown in controlled environments for *O. Universa* are taken from Sanyal et al. (1996); data for *G. Sacculifer* are taken from Sanyal et al. (2001), and data for *G. Ruber* are taken from Henehan et al. (2013).

rate ion in solution (e.g., Hönisch et al., 2004; Krief et al., 2010; Henehan et al., 2013) and their $\delta^{11}B$ is often less sensitive to pH than the aqueous borate ion (e.g., Hönisch et al., 2004). Although a small number of species has been investigated so far, the data call for clear "vital" effects. The main vital effect that has been invoked to explain why biogenic carbonates are more enriched in ^{11}B than borate in solution is an increase of the fluid pH at the calcification sites of corals (e.g., Rollion-Bard et al., 2011b; Trotter et al., 2011; Anagnostou et al., 2012) and foraminifera (e.g., Rollion-Bard and Erez, 2010). This hypothesis is confirmed by in situ measurements of pH using microelectrodes, both in foraminifera (e.g., Jørgensen et al., 1985) and in corals (e.g., Venn et al., 2013).

Although our results from inorganic experiments cannot be directly used to interpret $\delta^{11}B$ measured in biogenic carbonates, they are interesting for comparison with the results of culture experiments. The most striking difference between the published data on biogenic carbonate and the result of this study on inorganically precipitated carbonates is the opposite $\delta^{11}B$ behavior with respect to the mineral phase. Although the inorganic data of this study show a larger fractionation of boron isotopes in aragonite compared with calcite (at all pH values), the reverse is observed in biogenic carbonates. Nevertheless, our results confirm that any biologically driven increase of pH at the calcification site of aragonitic organisms will result in an increased $\delta^{11}B$ compared with the $\delta^{11}B$ of seawater borate. Based on our data, we deduce that aragonite corals should increase their internal pH by ~1 pH unit at the site of calcification if all parameters are held constant. This observation is confirmed by direct measurements of pH in the subcalicoblastic medium (Venn et al., 2013). In contrast, a simple calcifying mechanism in which the only difference between biogenic and inorganic calcite is a local pH increase cannot explain $\delta^{11}B$ in biogenic calcite (Fig. 8). This shows that differences in boron aqueous speciation and growth mechanisms between biogenic and inorganic carbonates could play an important role in the $\delta^{11}B$ value of carbonates and in its dependency on pH. For example, extracellular exudates produced by the organisms (e.g., Gower and Tirrell, 1998) could form strong complexes with aqueous borate. Aqueous borate is known to form strong complexes with aliphatic and aromatic carboxylic acids or phenols and these complexes are fractionated toward heavier values than aqueous borate ion (Lemarchand, 2005). This could make aqueous borate and thus precipitating $CaCO_3$ enriched in ^{11}B compared to $CaCO_3$ formed in organic-free solutions. Alternatively, B-organic complexes in which B–O bonds lengths are longer than in aqueous borate will lead to a ^{10}B enrichment of $CaCO_3$ compared to inorganic $CaCO_3$.

On the other hand, a possible insight on complex calcifying processes could be provided from octocorals that produce calcite instead of aragonite. In the calcite-precipitating coral *Corallium* sp., McCulloch et al. (2012) showed that $\delta^{11}B$ resembles the borate curve of seawater. Although the calcifying mechanism of this organism is still not fully understood, a recent study evidenced the presence of an extracellular protein (called ECMP-67) that drives the precipitation of calcite instead of aragonite not only in the *L. crassum* octocoral but also in inorganic experiments that should have otherwise resulted in aragonite precipitation (Rahman et al., 2011). Investigation of the effect of such a protein that offers an alternative to the internal pH increase effect that is usually invoked to explain natural $\delta^{11}B$ data could provide a better understanding of both the calcifying mechanisms and the impact of boron aqueous speciation in biological organisms.

By showing that inorganic calcite can be enriched in ^{11}B due to the incorporation of boric acid from the solution, our experiments suggest that boric acid is likely to be incorporated into the crystal during the biological precipitations of carbonates. This incorporation could thus contribute (in addition to such other mechanisms as a local pH increase and change in B speciation) to the high $\delta^{11}B$ values observed in biogenic carbonates. This conclusion was reached by Rollion-Bard et al. (2011a) based on ion microprobe $\delta^{11}B$ measurements coupled with boron speciation data in *Lophelia pertusa* deep-sea coral.

The result of our NMR measurements in inorganic calcite and aragonite also differs significantly from those in biological calcite and aragonite. Unlike our study, Klochko et al. (2009) found no evidence of dependency of boron coordination on crystal structure and observed similar proportions of both BO_3 and BO_4 in the calcite and aragonite of modern foraminifera and corals, respectively. Although their results are compatible with a change of coordination during B uptake, it appears that in addition to a pH increase at aragonite growth sites, aqueous boric acid could be incorporated to account for the high BO_3 proportions in the coral and for a portion of the $\delta^{11}B$ offset. The second possibility is that the extent of the change of coordination could be higher in biological aragonite, perhaps in relation to the coral precipitation rate. Finally, based on synchrotron X-ray spectrometry, Branson et al. (2015) evidenced the sole presence of trigonal boron in the calcite of *Amphistegina lessonii* foraminifera, again showing that a coordination change exists but that the controls on B speciation in biogenic calcite still remain to be identified.

5. Conclusions

The proposed mechanisms of boron incorporation into inorganic calcite and aragonite inferred from the current study are shown in Fig. 9. In inorganic aragonite, boron incorporation is consistent with the preferential incorporation of borate without isotope fractionation. In the solid, a marginal change of coordination from BO_4 to BO_3 occurs but does not influence the $\delta^{11}B$ of aragonite. In calcite, even if the possibility of the incorporation of borate only with an isotopic fractionation is not entirely ruled out, the incorporation of both boric acid and borate with no isotope fractionation gives a satisfactory description of our experimental data. The fraction of boric acid directly incorporated in calcite is correlated to the fractions of aqueous boric acid, which decrease from 30% to 15% when the solution pH is raised from 7.5 to 8.9. Despite the uncertainties in the exact structure and stoichiometry of the boron species attached to the carbonate surface and incorporated in the lattice, our data clearly indicate a strong control of the crystal structure on the boron isotopic fractionation between

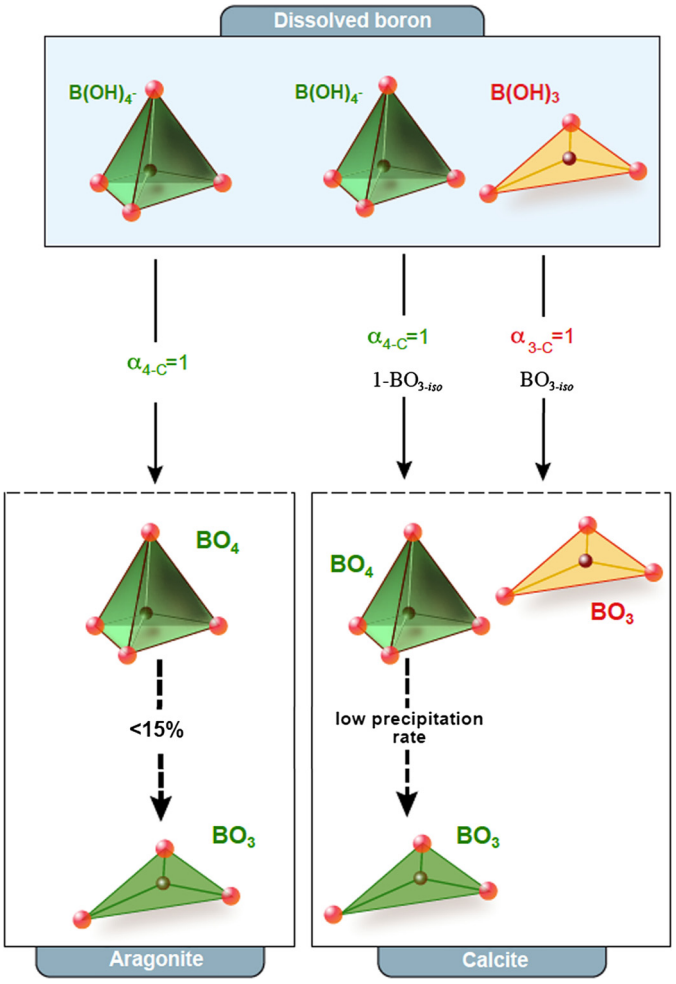

Fig. 9. Conceptual model of boron incorporation in aragonite and calcite suggested from both isotopic and NMR data. In aragonite, aqueous borate is the only species incorporated with no isotope fractionation ($\alpha_{4\text{-}C} = 1$). A change of coordination explains the small amount of BO_3 in the solid. In calcite, both aqueous borate and boric acid are incorporated assuming no fractionation between solution and solid ($\alpha_{4\text{-}C} = 1$ and $\alpha_{3\text{-}C} = 1$). The difference between the proportions of trigonal boron incorporated in the solid calculated by isotope mass budget ($BO_{3\text{-}ISO}$, Eq. (2)) or measured by NMR implies that a coordination change from tetrahedral to trigonal species occurs in calcite and preferentially at low precipitation rate.

the solution and calcium carbonates. We show that the mechanism controlling B incorporation in inorganic $CaCO_3$ is much simpler for aragonite than for calcite, and in aragonite, $\delta^{11}B$ is more sensitive to solution pH variations than in calcite.

Overall, the current study of boron inorganic co-precipitation with calcite and aragonite, which is the first study to use coupled ^{11}B MAS NMR and isotopic data over a wide range of solution pH and $CaCO_3$ precipitation rates, clearly demonstrates crystallographic control of boron isotopic composition in calcium carbonates in addition to the expected control by the pH of the parent solution. This study has implications on the paleo-pH proxy understanding because our results showed that boron incorporation in aragonite follows the hypothesis of borate incorporation used to reconstruct ocean paleo-acidities, as proposed by Hemming and Hanson (1992), while calcite does not follow this hypothesis. In calcite, the boron isotope composition remains dependent on pH and thus suitable for pH reconstructions, although it appears less sensitive to pH than in aragonite, a feature observed in biogenic carbonates as well. Although pH increase in biogenic carbonates may explain the $\delta^{11}B$ in biogenic aragonite compared to inorganic aragonite, specific vital effects, like the excretion of boron-complexing organic exudates, probably control the $\delta^{11}B$ of biogenic calcite. Importantly, this study highlights the possibility of direct incorporation of significant amounts of boric acid in biogenic carbonates. The accurate use of calcite $\delta^{11}B$ for paleo-pH reconstructions will require further theoretical and experimental work to characterize the exact mechanisms of B incorporation and isotope fractionation in this mineral.

Acknowledgement

The authors thank J. Bouchez for advice during manuscript preparation and J. Dyon for greatly improving the figures. This work acknowledges funding by the TGIR-RMN-THC Fr3050 CNRS (NMR spectra acquisition), the French National Research Agency through the CARBORIC (ANR-13-BS06-0013-02) project and French Ministry of Education and Research though JN thesis grant. We thank Katherine Allen and two anonymous reviewers for constructive comments. This is IPGP contribution number 3646.

Appendix A. Supplementary material

Supplementary material related to this article can be found online at http://dx.doi.org/10.1016/j.epsl.2015.07.063.

References

Anagnostou, E., Huang, K.-F., You, C.-F., Sikes, E.L., Sherrell, R.M., 2012. Evaluation of boron isotope ratio as a pH proxy in the deep sea coral Desmophyllum dianthus: evidence of physiological pH adjustment. Earth Planet. Sci. Lett. 349–350, 251–260. http://dx.doi.org/10.1016/j.epsl.2012.07.006.

Baes, C.F., Mesmer, R.E., 1976. The Hydrolysis of Cations. John Wiley & Sons, New York.

Bates, R.G., 1973. Determination of pH: Theory and Practice. John Wiley & Sons, New York.

Blamart, D., Rollion-Bard, C., Meibom, A., Cuif, J.-P., Juillet-Leclerc, A., Dauphin, Y., 2007. Correlation of boron isotopic composition with ultrastructure in the deep-sea coral Lophelia pertusa: implications for bio-mineralization and paleo-pH. Geochem. Geophys. Geosyst. 8, 11. http://dx.doi.org/10.1029/2007GC001686.

Branson, O., Kaczmarek, K., Redfern, S.A.T., Misra, S., Langer, G., Tyliszczak, T., Bijma, J., Elderfield, H., 2015. The coordination and distribution of B in foraminiferal calcite. Earth Planet. Sci. Lett. 416, 67–72. http://dx.doi.org/10.1016/j.epsl.2015.02.006.

Dandurand, J.L., Gout, R., Hoefs, J., Menschel, G., Schott, J., Usdowski, E., 1982. Kinetically controlled variations of major components and carbon and oxygen isotopes in a calcite-precipitating spring. Chem. Geol. 36, 299–315. http://dx.doi.org/10.1016/0009-2541(82)90053-5.

Dickson, A.G., 1990. Thermodynamics of the dissociation of boric acid in synthetic seawater from 273.15 to 318.15 K. Deep-Sea Res., A, Oceanogr. Res. Pap. 37, 755–766. http://dx.doi.org/10.1016/0198-0149(90)90004-F.

Douville, E., Paterne, M., Cabioch, G., Louvat, P., Gaillardet, J., Juillet-Leclerc, A., Ayliffe, L., 2010. Abrupt sea surface pH change at the end of the Younger Dryas in the central sub-equatorial Pacific inferred from boron isotope abundance in corals (Porites). Biogeosciences 7, 2445–2459. http://dx.doi.org/10.5194/bg-7-2445-2010.

Foster, G.L., 2008. Seawater pH, pCO_2 and $[CO^{2-}{}_3]$ variations in the Caribbean Sea over the last 130 kyr: a boron isotope and B/Ca study of planktic foraminifera. Earth Planet. Sci. Lett. 271, 254–266. http://dx.doi.org/10.1016/j.epsl.2008.04.015.

Foster, G.L., Hönisch, B., Paris, G., Dwyer, G.S., Rae, J.W.B., Elliott, T., Gaillardet, J., Hemming, N.G., Louvat, P., Vengosh, A., 2013. Interlaboratory comparison of boron isotope analyses of boric acid, seawater and marine $CaCO_3$ by MC-ICPMS and NTIMS. Chem. Geol. 358, 1–14. http://dx.doi.org/10.1016/j.chemgeo.2013.08.027.

Gabitov, R.I., Rollion-Bard, C., Tripati, A., Sadekov, A., 2014. In situ study of boron partitioning between calcite and fluid at different crystal growth rates. Geochim. Cosmochim. Acta 137, 81–92. http://dx.doi.org/10.1016/j.gca.2014.04.014.

Gower, L.A., Tirrell, D.A., 1998. Calcium carbonate films and helices grown in solutions of poly(aspartate). J. Cryst. Growth 191, 153–160. http://dx.doi.org/10.1016/S0022-0248(98)00002-5.

Gussone, N., Böhm, F., Eisenhauer, A., Dietzel, M., Heuser, A., Teichert, B.M.A., Reitner, J., Wörheide, G., Dullo, W.-C., 2005. Calcium isotope fractionation in calcite and aragonite. Geochim. Cosmochim. Acta 69, 4485–4494. http://dx.doi.org/10.1016/j.gca.2005.06.003.

Hemming, N., Hanson, G., 1992. Boron isotopic composition and concentration in modern marine carbonates. Geochim. Cosmochim. Acta 56, 537–543.

Hemming, N.G., Reeder, R.J., Hanson, G.N., 1995. Mineral–fluid partitioning and isotopic fractionation of boron in synthetic calcium carbonate. Geochim. Cosmochim. Acta 59, 371–379. http://dx.doi.org/10.1016/0016-7037(95)00288-B.

Henehan, M.J., Rae, J.W.B., Foster, G.L., Erez, J., Prentice, K.C., Kucera, M., Bostock, H.C., Martínez-Botí, M.A., Milton, J.A., Wilson, P.A., Marshall, B.J., Elliott, T., 2013. Calibration of the boron isotope proxy in the planktonic foraminifera Globigerinoides ruber for use in palaeo-CO_2 reconstruction. Earth Planet. Sci. Lett. 364, 111–122. http://dx.doi.org/10.1016/j.epsl.2012.12.029.

Hönisch, B., Bijma, J., Russell, A.D., Spero, H.J., Palmer, M.R., Zeebe, R.E., Eisenhauer, A., 2003. The influence of symbiont photosynthesis on the boron isotopic composition of foraminifera shells. Mar. Micropaleontol. 49, 87–96. http://dx.doi.org/10.1016/S0377-8398(03)00030-6.

Hönisch, B., Hemming, N.G., Grottoli, A.G., Amat, A., Hanson, G.N., Bijma, J., 2004. Assessing scleractinian corals as recorders for paleo-pH: empirical calibration and vital effects. Geochim. Cosmochim. Acta 68, 3675–3685. http://dx.doi.org/10.1016/j.gca.2004.03.002.

Hönisch, B., Hemming, N.G., 2005. Surface ocean pH response to variations in pCO_2 through two full glacial cycles. Earth Planet. Sci. Lett. 236, 305–314. http://dx.doi.org/10.1016/j.epsl.2005.04.027.

Jørgensen, B.B., Erez, J., Revsbech, P., Cohen, Y., 1985. Symbiotic photosynthesis in a planktonic foraminiferan, Globigerinoides sacculifer (Brady), studied with microelectrodes 1. Limnol. Oceanogr. 30, 1253–1267. http://dx.doi.org/10.4319/lo.1985.30.6.1253.

Klochko, K., Kaufman, A.J., Yao, W., Byrne, R.H., Tossell, J.A., 2006. Experimental measurement of boron isotope fractionation in seawater. Earth Planet. Sci. Lett. 248, 276–285. http://dx.doi.org/10.1016/j.epsl.2006.05.034.

Klochko, K., Cody, G.D., Tossell, J.A., Dera, P., Kaufman, A.J., 2009. Re-evaluating boron speciation in biogenic calcite and aragonite using ^{11}B MAS NMR. Geochim. Cosmochim. Acta 73, 1890–1900. http://dx.doi.org/10.1016/j.gca.2009.01.002.

Krief, S., Hendy, E.J., Fine, M., Yam, R., Meibom, A., Foster, G.L., Shemesh, A., 2010. Physiological and isotopic responses of scleractinian corals to ocean acidification. Geochim. Cosmochim. Acta 74, 4988–5001. http://dx.doi.org/10.1016/j.gca.2010.05.023.

Lemarchand, E., 2005. Etude des mécanismes de fractionnement isotopique du bore lors de son interaction avec les acides humiques et les oxydes de fer et manganese. PhD thesis. Paul-Sabatier University, Toulouse, 177 pp.

Lemarchand, E., Schott, J., Gaillardet, J., 2005. Boron isotopic fractionation related to boron sorption on humic acid and the structure of surface complexes formed. Geochim. Cosmochim. Acta 69, 3519–3533. http://dx.doi.org/10.1016/j.gca.2005.02.024.

Lemarchand, E., Schott, J., Gaillardet, J., 2007. How surface complexes impact boron isotope fractionation: evidence from Fe and Mn oxides sorption experiments. Earth Planet. Sci. Lett. 260, 277–296. http://dx.doi.org/10.1016/j.epsl.2007.05.039.

Louvat, P., Bouchez, J., Paris, G., 2010. MC-ICP-MS isotope measurements with direct injection nebulisation (d-DIHEN): optimisation and application to boron in seawater and carbonate samples. Geostand. Geoanal. Res. 35, 75–88. http://dx.doi.org/10.1111/j.1751-908X.2010.00057.x.

Louvat, P., Moureau, J., Paris, G., Bouchez, J., Noireaux, J., Gaillardet, J., 2014. A fully automated direct injection nebulizer (d-DIHEN) for MC-ICP-MS isotope analysis: application to boron isotope ratio measurements. J. Anal. At. Spectrom. 29, 1698–1707. http://dx.doi.org/10.1039/c4ja00098f.

Martell, A.E., Smith, R., Motekaitis, R.J., 2004. NIST critically selected stability constants of metal complexes. NIST Stand. Ref. Database 46.

Mavromatis, V., Gautier, Q., Bosc, O., Schott, J., 2013. Kinetics of Mg partition and Mg stable isotope fractionation during its incorporation in calcite. Geochim. Cosmochim. Acta 114, 188–203. http://dx.doi.org/10.1016/j.gca.2013.03.024.

Mavromatis, V., Montouillout, V., Noireaux, J., Gaillardet, J., Schott, J., 2015. Characterization of boron incorporation and speciation in calcite and aragonite from co-precipitation experiments under controlled pH, temperature and precipitation rate. Geochim. Cosmochim. Acta 150, 299–313. http://dx.doi.org/10.1016/j.gca.2014.10.024.

McCulloch, M., Trotter, J., Montagna, P., Falter, J., Dunbar, R., Freiwald, A., Försterra, G., Correa, M.L., Maier, C., Rüggeberg, A., Taviani, M., 2012. Resilience of cold-water scleractinian corals to ocean acidification: boron isotopic systematics of pH and saturation state up-regulation. Geochim. Cosmochim. Acta. http://dx.doi.org/10.1016/j.gca.2012.03.027.

Nir, O., Vengosh, A., Harkness, J.S., Dwyer, G.S., Lahav, O., 2015. Direct measurement of the boron isotope fractionation factor: reducing the uncertainty in reconstructing ocean paleo-pH. Earth Planet. Sci. Lett. 414, 1–5. http://dx.doi.org/10.1016/j.epsl.2015.01.006.

Paris, G., Bartolini, A., Donnadieu, Y., Beaumont, V., Gaillardet, J., 2010. Investigating boron isotopes in a middle Jurassic micritic sequence: primary vs. diagenetic signal. Chem. Geol. 275, 117–126. http://dx.doi.org/10.1016/j.chemgeo.2010.03.013.

Parkhurst, D.L., Appelo, C.A.J., 2013. Description of input and examples for PHREEQC version 3: a computer program for speciation, batch-reaction, one-dimensional transport, and inverse geochemical calculations (USGS Numbered Series No. 6-A43). In: Techniques and Methods, U.S. Geological Survey. Reston, VA.

Pitzer, K.S., 1973. Thermodynamics of electrolytes. I. Theoretical basis and general equations. J. Phys. Chem. 77, 268–277. http://dx.doi.org/10.1021/j100621a026.

Pokrovski, G.S., Schott, J., Sergeyev, A.S., 1995. Experimental determination of the stability constants of $NaSO_4^-$ and $NaB(OH)_{40}$ in hydrothermal solutions using a new high-temperature sodium-selective glass electrode — implications for boron isotopic fractionation. Chem. Geol. 124, 253–265. http://dx.doi.org/10.1016/0009-2541(95)00057-S.

Rae, J.W.B., Foster, G.L., Schmidt, D.N., Elliott, T., 2011. Boron isotopes and B/Ca in benthic foraminifera: proxies for the deep ocean carbonate system. Earth Planet. Sci. Lett. 302, 403–413. http://dx.doi.org/10.1016/j.epsl.2010.12.034.

Rahman, M.A., Oomori, T., Wörheide, G., 2011. Calcite formation in soft coral sclerites is determined by a single reactive extracellular protein. J. Biol. Chem. 286, 31638–31649. http://dx.doi.org/10.1074/jbc.M109.070185.

Reynaud, S., Hemming, N.G., Juillet-Leclerc, A., Gattuso, J.-P., 2004. Effect of pCO_2 and temperature on the boron isotopic composition of the zooxanthellate coral Acropora sp. Coral Reefs. http://dx.doi.org/10.1007/s00338-004-0399-5.

Rollion-Bard, C., Erez, J., 2010. Intra-shell boron isotope ratios in the symbiont-bearing benthic foraminiferan Amphistegina lobifera: implications for δ^{11}B vital effects and paleo-pH reconstructions. Geochim. Cosmochim. Acta 74, 1530–1536. http://dx.doi.org/10.1016/j.gca.2009.11.017.

Rollion-Bard, C., Blamart, D., Trebosc, J., Tricot, G., Mussi, A., Cuif, J.-P., 2011a. Boron isotopes as pH proxy: a new look at boron speciation in deep-sea corals using ^{11}B MAS NMR and EELS. Geochim. Cosmochim. Acta 75, 1003–1012. http://dx.doi.org/10.1016/j.gca.2010.11.023.

Rollion-Bard, C., Chaussidon, M., France-Lanord, C., 2011b. Biological control of internal pH in scleractinian corals: implications on paleo-pH and paleo-temperature reconstructions. C. R. Géosci. 343, 397–405. http://dx.doi.org/10.1016/j.crte.2011.05.003.

Ruiz-Agudo, E., Putnis, C.V., Kowacz, M., Ortega-Huertas, M., Putnis, A., 2012. Boron incorporation into calcite during growth: implications for the use of boron in carbonates as a pH proxy. Earth Planet. Sci. Lett. 345–348, 9–17. http://dx.doi.org/10.1016/j.epsl.2012.06.032.

Sanyal, A., Hemming, N.G., Broecker, W.S., Lea, D.W., Spero, H.J., Hanson, G.N., 1996. Oceanic pH control on the boron isotopic composition of foraminifera: evidence from culture experiments. Paleoceanography 11, 513–517. http://dx.doi.org/10.1029/96PA01858.

Sanyal, A., Nugent, M., Reeder, R.J., Bijma, J., 2000. Seawater pH control on the boron isotopic composition of calcite: evidence from inorganic calcite precipitation experiments. Geochim. Cosmochim. Acta 64, 1551–1555. http://dx.doi.org/10.1016/S0016-7037(99)00437-8.

Sanyal, A., Bijma, J., Spero, H., Lea, D.W., 2001. Empirical relationship between pH and the boron isotopic composition of Globigerinoides sacculifer: implications for the boron isotope paleo-pH proxy. Paleoceanography 16, 515–519. http://dx.doi.org/10.1029/2000PA000547.

Sen, S., Stebbins, J.F., 1994. Coordination environments of B impurities in calcite and aragonite polymorphs: a ^{11}B MAS NMR study. Am. Mineral. 79, 819–825.

Tang, J., Dietzel, M., Böhm, F., Köhler, S.J., Eisenhauer, A., 2008. Sr^{2+}/Ca^{2+} and $^{44}Ca/^{40}Ca$ fractionation during inorganic calcite formation: II. Ca isotopes. Geochim. Cosmochim. Acta 72, 3733–3745. http://dx.doi.org/10.1016/j.gca.2008.05.033.

Tossell, J.A., 2006. Boric acid adsorption on humic acids: ab initio calculation of structures, stabilities, ^{11}B NMR and ^{11}B, ^{10}B isotopic fractionations of surface complexes. Geochim. Cosmochim. Acta 70, 5089–5103. http://dx.doi.org/10.1016/j.gca.2006.08.014.

Trotter, J., Montagna, P., McCulloch, M., Silenzi, S., Reynaud, S., Mortimer, G., Martin, S., Ferrier-Pagès, C., Gattuso, J.-P., Rodolfo-Metalpa, R., 2011. Quantifying the pH 'vital effect' in the temperate zooxanthellate coral Cladocora caespitosa: validation of the boron seawater pH proxy. Earth Planet. Sci. Lett. 303, 163–173. http://dx.doi.org/10.1016/j.epsl.2011.01.030.

Uchikawa, J., Penman, D.E., Zachos, J.C., Zeebe, R.E., 2015. Experimental evidence for kinetic effects on B/Ca in synthetic calcite: implications for potential $B(OH)_4^-$ and $B(OH)_3$ incorporation. Geochim. Cosmochim. Acta 150, 171–191. http://dx.doi.org/10.1016/j.gca.2014.11.022.

Vengosh, A., Kolodny, Y., Starinsky, A., Chivas, A.R., McCulloch, M.T., 1991. Co-precipitation and isotopic fractionation of boron in modern biogenic carbonates. Geochim. Cosmochim. Acta 55, 2901–2910. http://dx.doi.org/10.1016/0016-7037(91)90455-E.

Venn, A.A., Tambutté, E., Holcomb, M., Laurent, J., Allemand, D., Tambutté, S., 2013. Impact of seawater acidification on pH at the tissue–skeleton interface and calcification in reef corals. Proc. Natl. Acad. Sci. 110, 1634–1639. http://dx.doi.org/10.1073/pnas.1216153110.

Von Allmen, K., Böttcher, M.E., Samankassou, E., Nägler, T.F., 2010. Barium isotope fractionation in the global barium cycle: first evidence from barium minerals and precipitation experiments. Chem. Geol. 277, 70–77. http://dx.doi.org/10.1016/j.chemgeo.2010.07.011.